Electronic Supplementary Material (ESI) for Soft Matter

Supporting Information

Non-amphiphilic pyrene cored poly(aryl ether) dendron based gels: tunable morphology, unusual solvent effects on the emission and fluoride ion detection by the self-assembled superstructures

P. Rajamalli and Edamana Prasad*

Department of Chemistry, Indian Institute of Technology Madras (IITM), Chennai 600 036, India

Email: pre@iitm.ac.in

Contents **Page Number**

1. Synthetic procedure and characterizations of dendrons

All compounds were synthesized according to reported procedures.[1, 2]

1.1.Synthesis of compound II

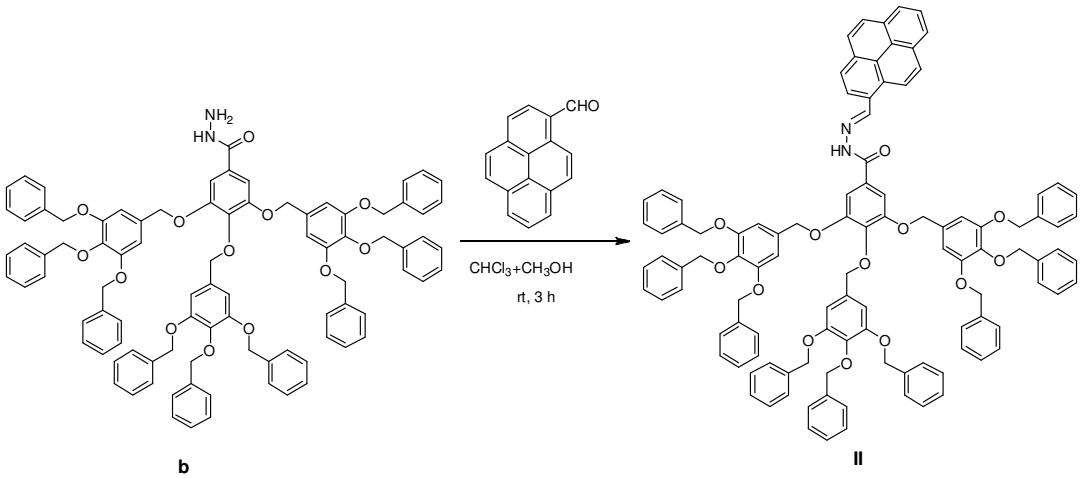

A solution of 1-pyrenecarboxaldehyde (0.16 g, 0.00071 mole) in methanol was added drop wise to a $CHCl_3$ solution of compound **b** (1 g, 0.00071 mole). The mixture was stirred for 3 hours. The resulting precipitate was filtered off by suction and dried under vacuum to yield **II** (1.05 g, 90.5 %); **^{1}H NMR (400 MHz, $CDCl_3$) δ**: 4.84-5.05 (m, ArC*H*$_2$O, 24H), 6.74-6.79 (m, Ar*H*, 6H), 7.21-7.36 (m, Ar*H* & Ph*H*, 47H), 7.99 (s, Py*H*, 3H), 8.09-8.14 (m, Py*H*, 3H), 8.12-8.19(d, *J* = 8 Hz, Py*H*, 1H), 8.71(s, Py*H*, 2H), 9.05 (s, C*H*=N, 1H), 9.15 (s, CON*H*, 1H); **^{13}C NMR (100 MHz, DMSO-d_6) δ:** 70.61, 70.82, 71.16, 74.88, 74.98, 106.98, 107.57,107. 61, 108. 74, 127.15, 127.55, 127.74, 128.13, 128.31, 128.46, 128.63,128.88, 128.95, 128.98, 130.24, 130.78, 131.12, 131.30, 131.77, 131.89, 133.84, 133.98, 134.80, 134.93, 137.25, 137.41, 148.36, 151.90, 152.54, 168.29; **MS** (MALDI-TOF): m/z Calcd for $C_{108}H_{88}N_2O_{13}$: 1620.62, found: 1660.14$[M+K]^+$.

1.2 Synthesis of compound III

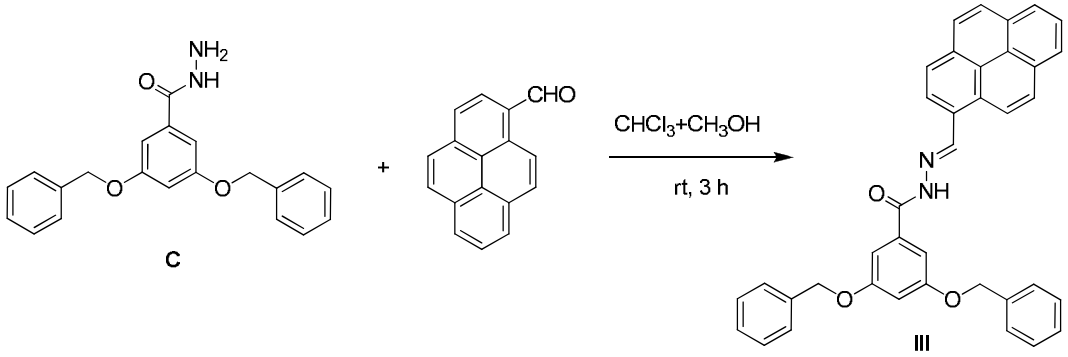

A solution of 1-pyrenecarboxaldehyde (0.66 g, 0.0029 mole) in methanol was added drop wise to a $CHCl_3$ solution of compound **c** (1 g, 0.0029 mole) under nitrogen atmosphere. The mixture was stirred for 3 hours. The resulting precipitate was filtered off by suction and dried under vacuum to yield **III** (1.56 g, 93.9 %); **^{1}H NMR (400 MHz, DMSO-d$_6$) δ**: 5.19 (s, ArC*H*$_2$O, 4H), 6.95 (s, Ar*H*, 1H), 7.26-7.49 (m, Ar*H* & PhH, 12H), 8.11 (t, Py*H*, *J* = 7.6 Hz, 1H), 8.24 (m, Py*H*, 2H), 8.35 (t, Py*H*, *J*= 8.0 Hz, 4H), 8.57 (d, Py*H*, *J*=8.0 Hz, 1H), 8.79 (d, Py*H*, *J* = 9.2 Hz, 1H), 9.51 (s, C*H*=N, 1H), 11.95(s, CON*H*, 1H); **^{13}C NMR (100 MHz, DMSO-d$_6$) δ:** 69.99, 103.29, 107.72, 124.24, 124.86, 125.08, 125.21, 125.56, 125.73, 126.90, 128.17, 128.31, 128.41, 128.07, 131.13, 131.75, 138.09,144.58, 159.58, 168.4; **HRMS (ES+)**: *m/z* Calcd for $C_{38}H_{28}N_2O_3$: 560.2100, found: 561.2189$[M+H]^+$.

1.3 Synthesis of compound IV

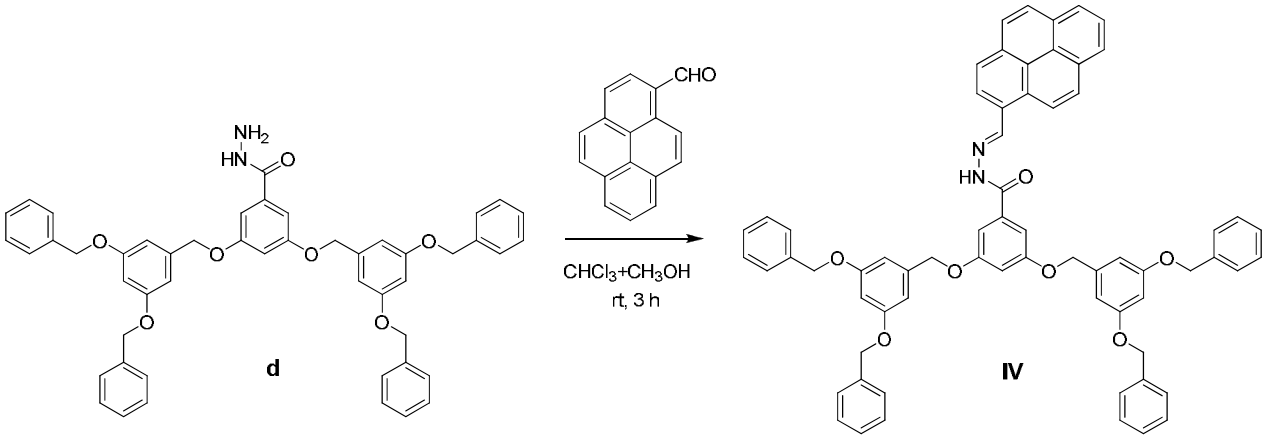

A solution of 1-pyrenecarboxaldehyde (0.298 g, 0.0013 mole) in methanol was added drop wise to a $CHCl_3$ solution of compound **d** (1 g, 0.0013 mole). The mixture was stirred for 3 hours. The

resulting precipitate was filtered off by suction and dried under vacuum to yield **IV** (1.2 g, 92.4 %); **^{1}H NMR (400 MHz, DMSO-d$_6$) δ:** 5.06 (s, ArC*H*$_2$O, 8H), 5.11 (s, ArC*H*$_2$O, 4H), 6.63 (s, Ar*H*, 2H), 6.73 (s, Ar*H*, 4H), 6.92 (s, Ar*H*, 1H), 7.23-7.42 (m, Ar*H* & Ph*H*, 22H), 8.19 (t, Py*H*, *J* = 6.0 Hz, 1H), 8.22 (m, Py*H*, 2H), 8.34 (t, Py*H*, *J* = 6.0 Hz, 4H), 8.57 (d, Py*H*, *J* = 8.0 Hz, 2H), 8.78 (d, Py*H*, *J* = 6.0 Hz, 2H), 9.50 (s, C*H*=N, 1H) 11.98 (s, CONH, 1H). **^{13}C NMR (100 MHz, DMSO-d$_6$) δ**: 70.28, 101.80, 106.56, 125.51, 126.20, 127.30, 127.70, 127.77, 127.96, 128.17, 128.37, 128.58, 128.73, 128.74, 129.09, 130.49, 131.39, 136.86, 139.00, 160.29, 160.35, 168. **MS** (MALDI-TOF): m/z Calcd for $C_{66}H_{52}N_2O_7$: 984.37, found: 1008.2[M+Na]$^+$, 1024.4[M+K]$^+$.

2. Plots of solvent parameters Vs CGC value

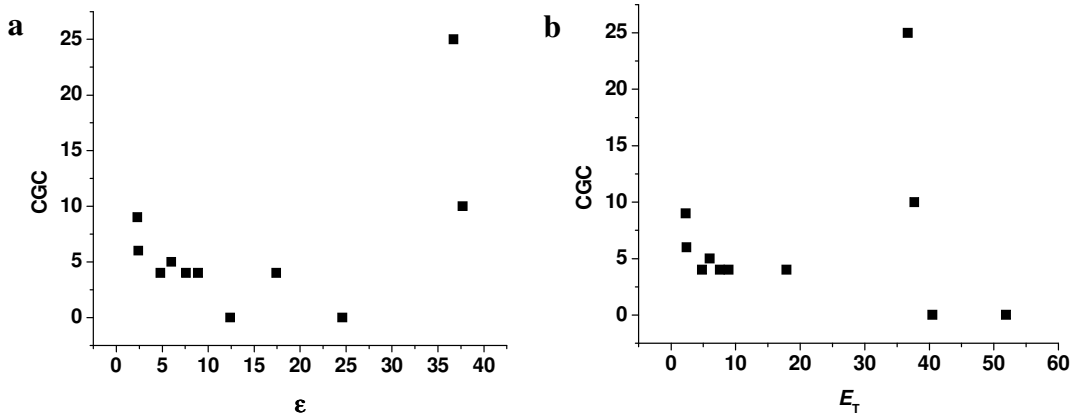

Fig. S1 Effect of solvent polarity parameters a) Dielectric constant (Є), and b) Reichart's parameter (E_T) on the CGC value for the compound **IV**.

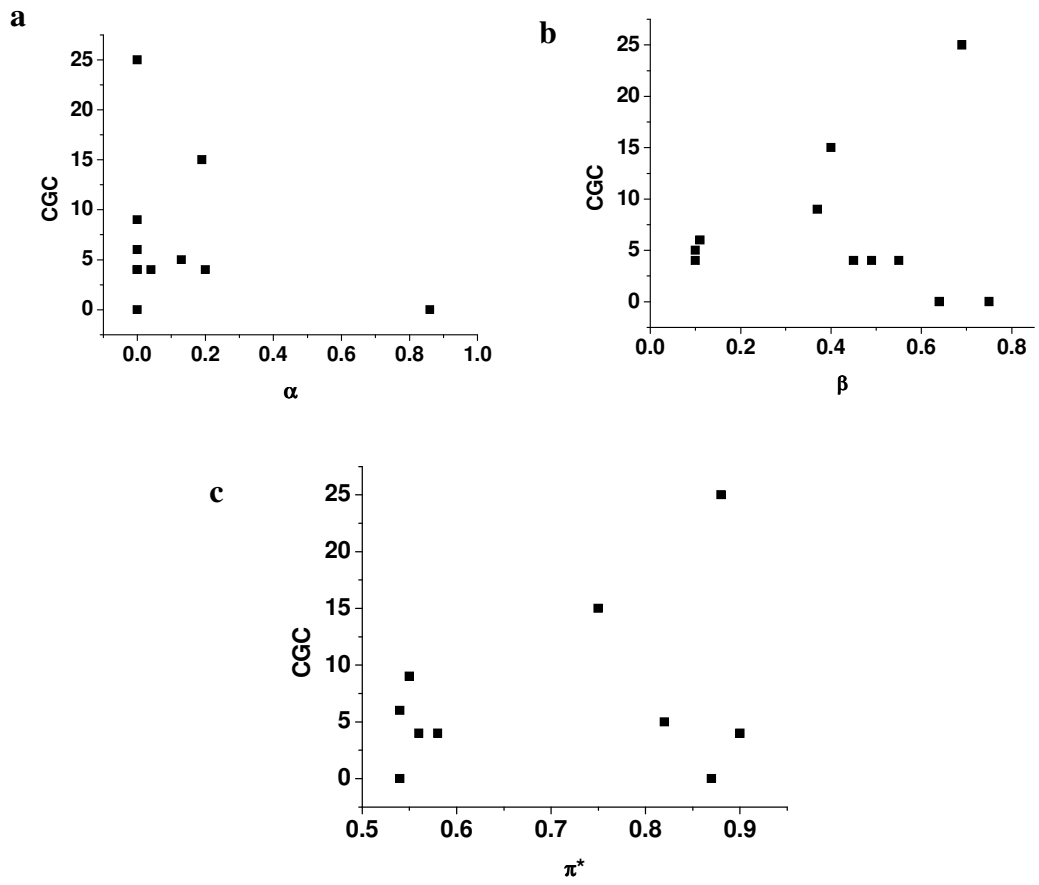

Fig. S2 Effect of individual Kamlet–Taft parameter on the CGC value for the compound **IV** CGC values a) α vs CGC, b) *β* vs CGC, and c) π* vs CGC.

3. FT-IR spectrum of gel

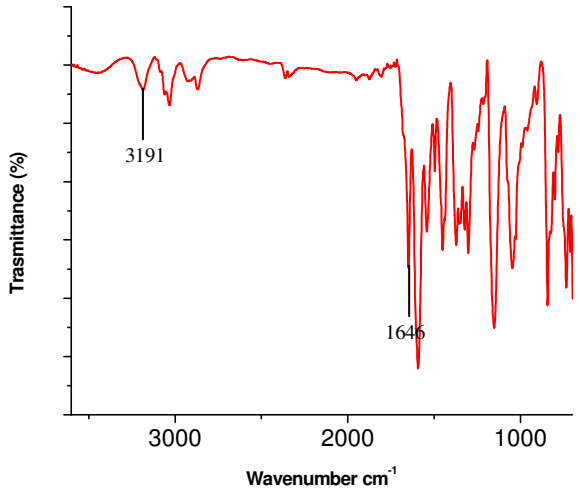

Fig. S3 FT-IR spectrum of the xerogel formed from compound **IV** in $CHCl_3$.

4. Powder-XRD Patterns

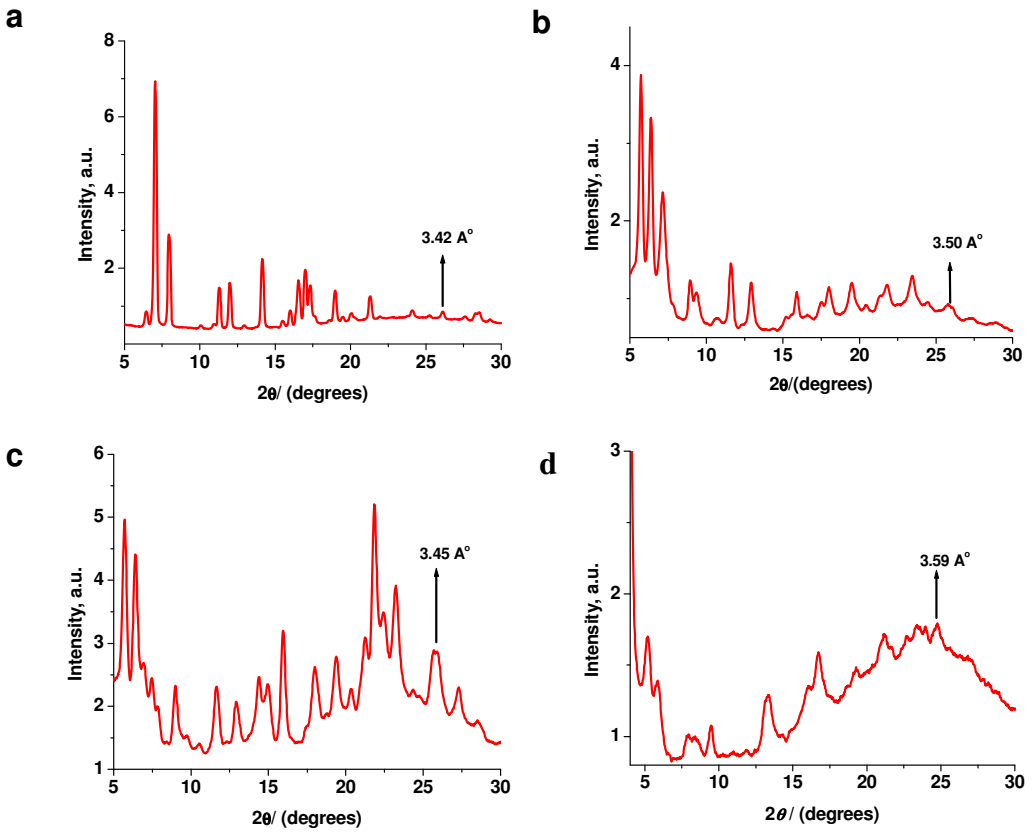

Fig. S4 Powder XRD pattern of xerogel formed from a) compound **I**, b) compound **II**, c) compound **III**, and d) compound **IV** in $CHCl_3$.

5. Plot of phase transition temperature vs concentration

The gel-sol phase transition temperature (T_{gel}) was estimated to be in between 53-63 ˚C in THF–water mixture (0.2-1.2 wt%). The gel transition temperature increases as the concentration of the gel increases. Plot shows the linear relation between the gel transition temperature and the gel concentration for the first generation AB_2 type dendron derivatives in THF–water mixture (1:1)

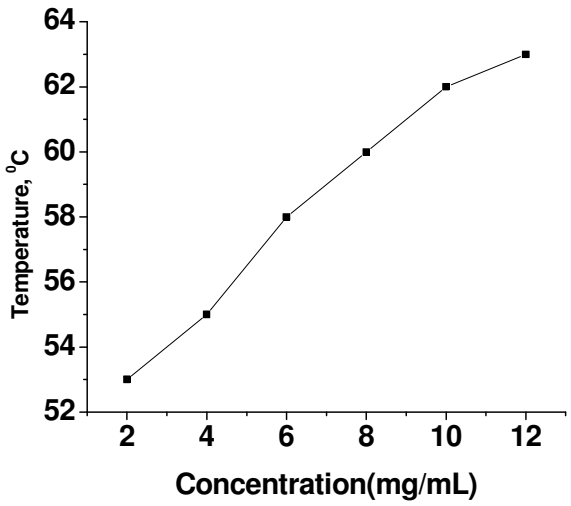

Fig. S5 Effect of concentration on the gel–sol phase-transition temperature (T_{gel}) of compound **III** in THF: water mixture, measured by ball droping method.

6. SEM images of xerogel and spherical aggregate

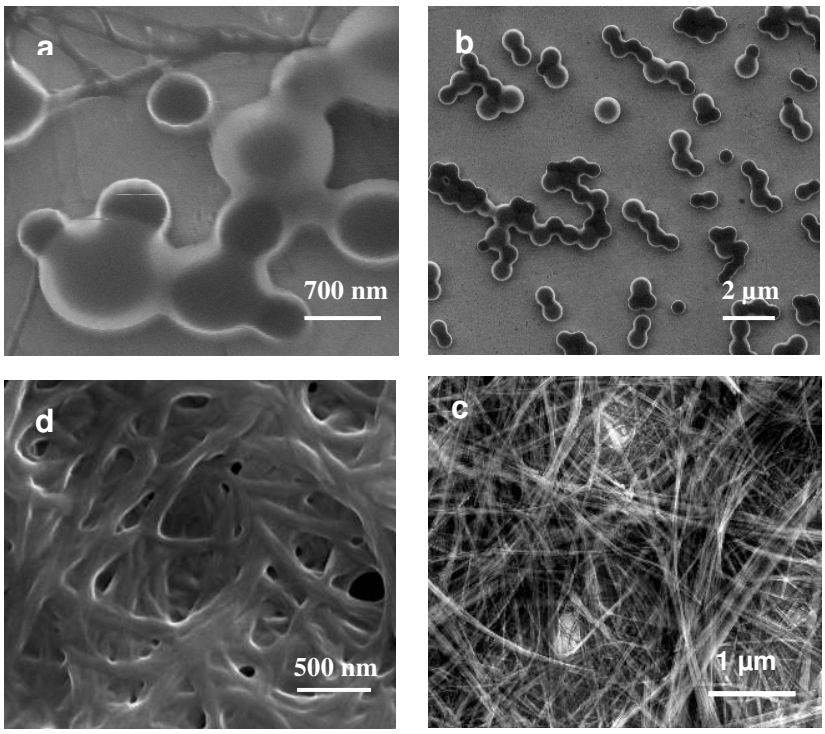

Fig. S6 SEM images of compound **IV**; a) larger vesicle formation from smaller vesicles in $CHCl_3$-MeOH, b) fibre formation from vesicles, c) finer formation in $CHCl_3$-hexane (above CGC), and d) fibre formation from compound **I** in THF-water.

7. Dynamic light scattering data

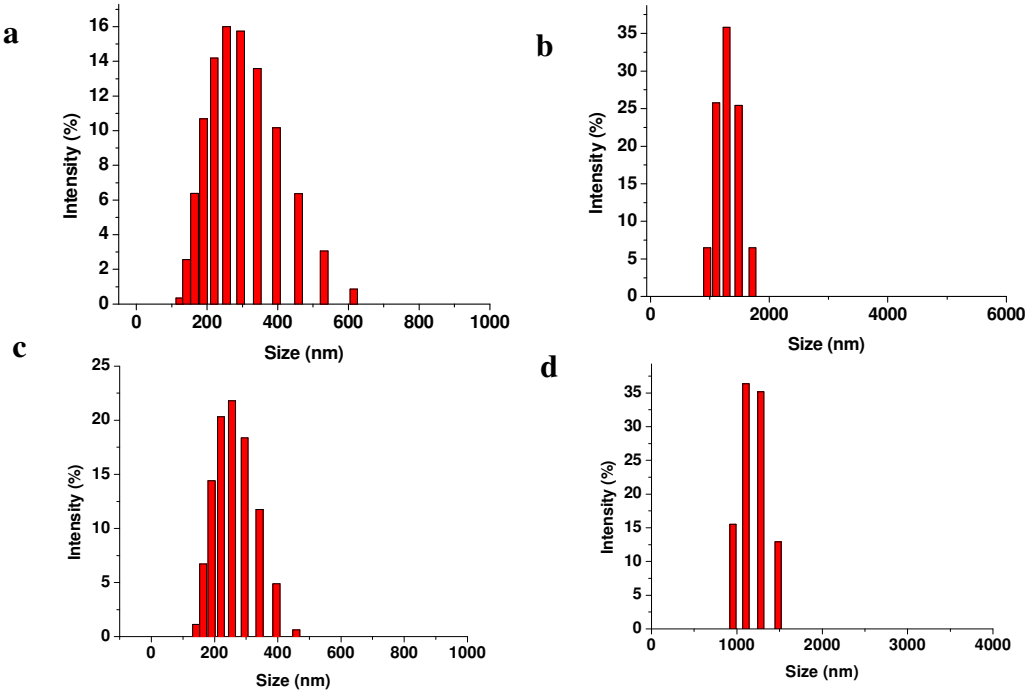

Fig. S7 Dynamic light scattering histograms of compounds **II** and **IV** in $CHCl_3$-MeOH (1: 1; v/v): [**II**] =[**IV**]= $1x10^{-5}$ M for (a) and (c), and [**II**] =[**IV**]= $1x10^{-4}$ M for (b) and (d).

7. AFM images of xerogel and spherical aggregates

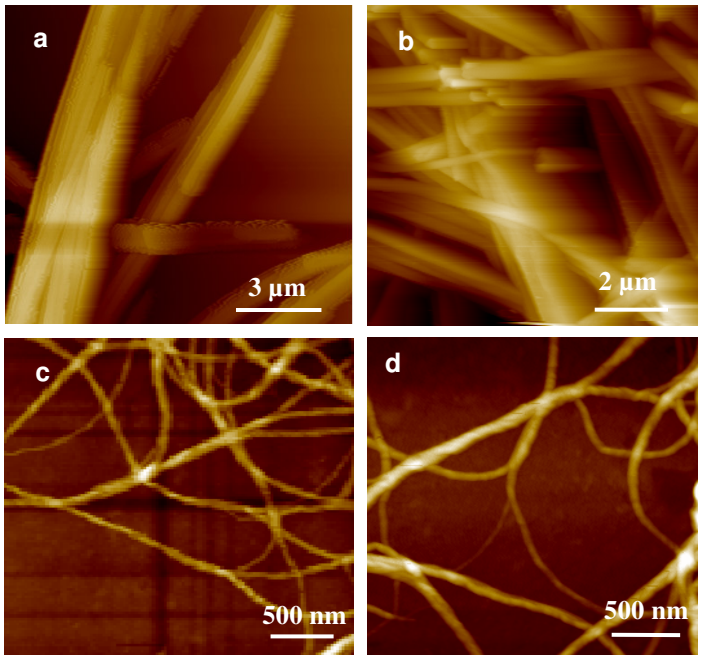

Fig. S8 AFM images of xerogel formed from a) compound **I,** b) compound **III,** c) compound **II** and d) **c**ompound **IV** in $CHCl_3$.

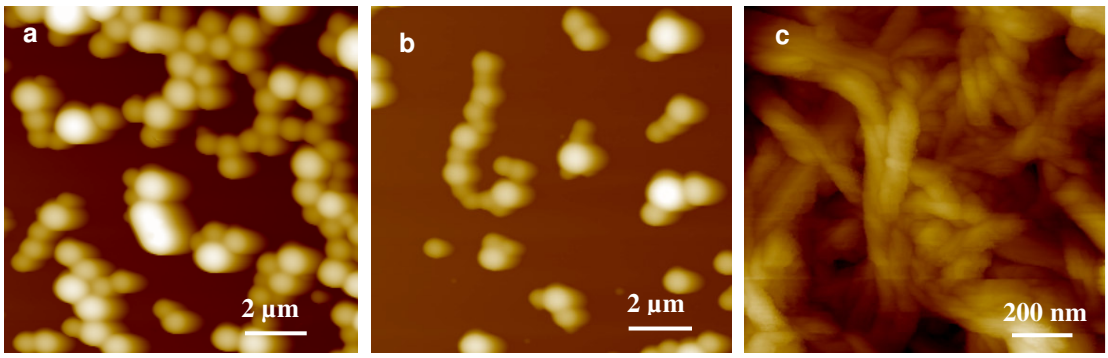

Fig. S9 AFM images of a) compound **II** in $CHCl_3$-MeOH (below CGC), b) vesicle to fibre conversion for compound **II**, and c) xerogel formed from compound **IV** in $CHCl_3$-hexane (above CGC).

8. AFM images of spiral and helical structure

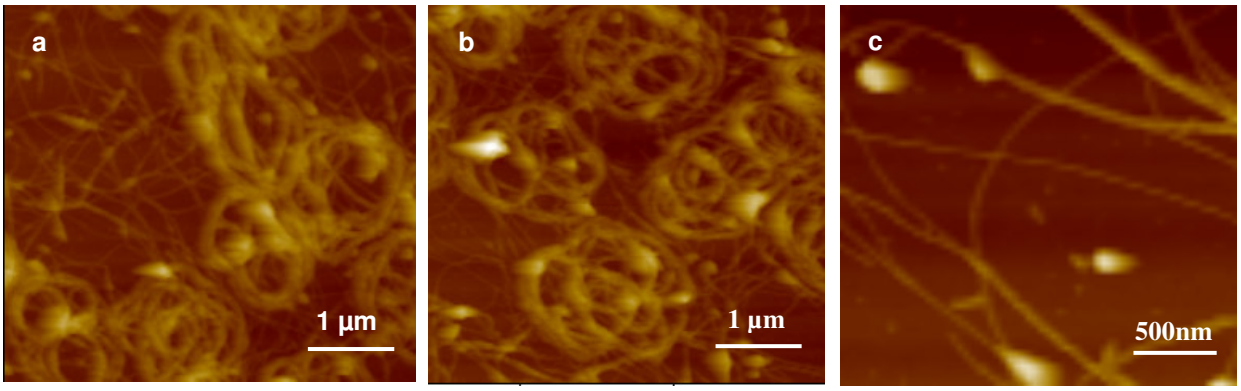

Fig. S10 AFM images of gel formed from toluene: a) compound **I**, b) compound **III**, and c) compound **II**.

9. CD spectrum

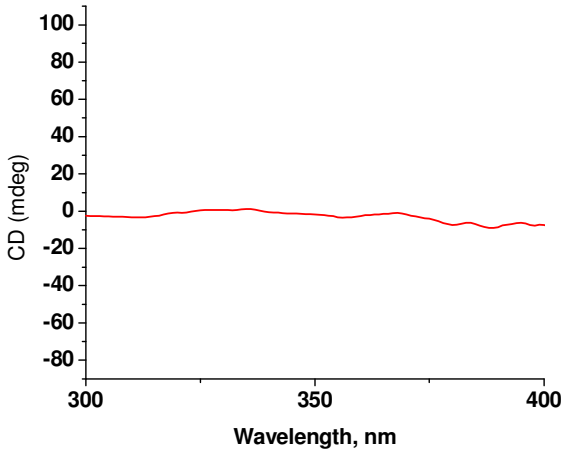

Fig. S11 CD spectrum of compound **I** in toluene.

10. TEM images of vesicles and gels

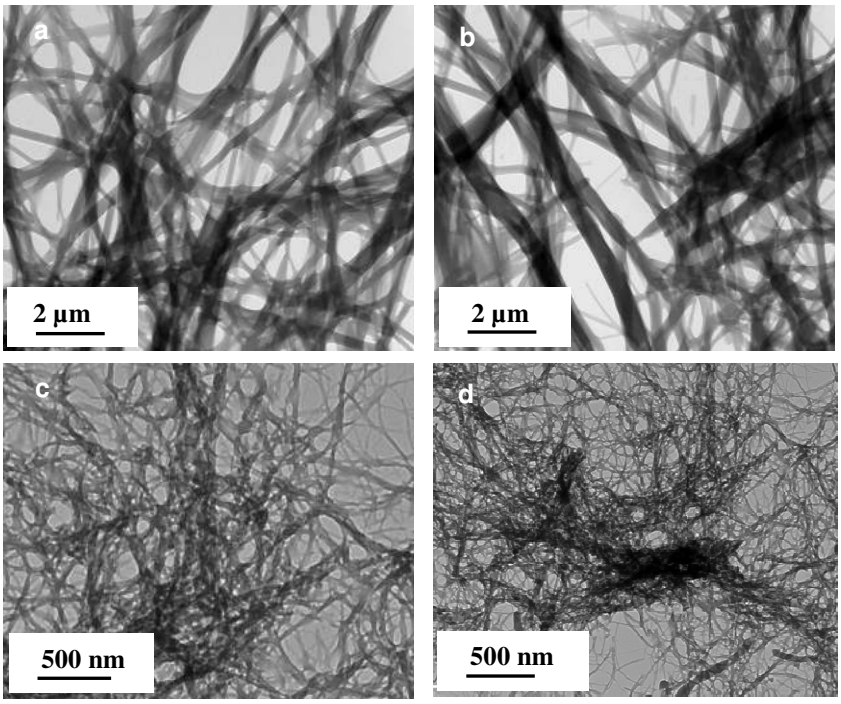

Fig. S12 TEM images of xerogel formed from a) compound **I,** b) compound **III,** c) compound **II** and d) compound **IV** in $CHCl_3$.

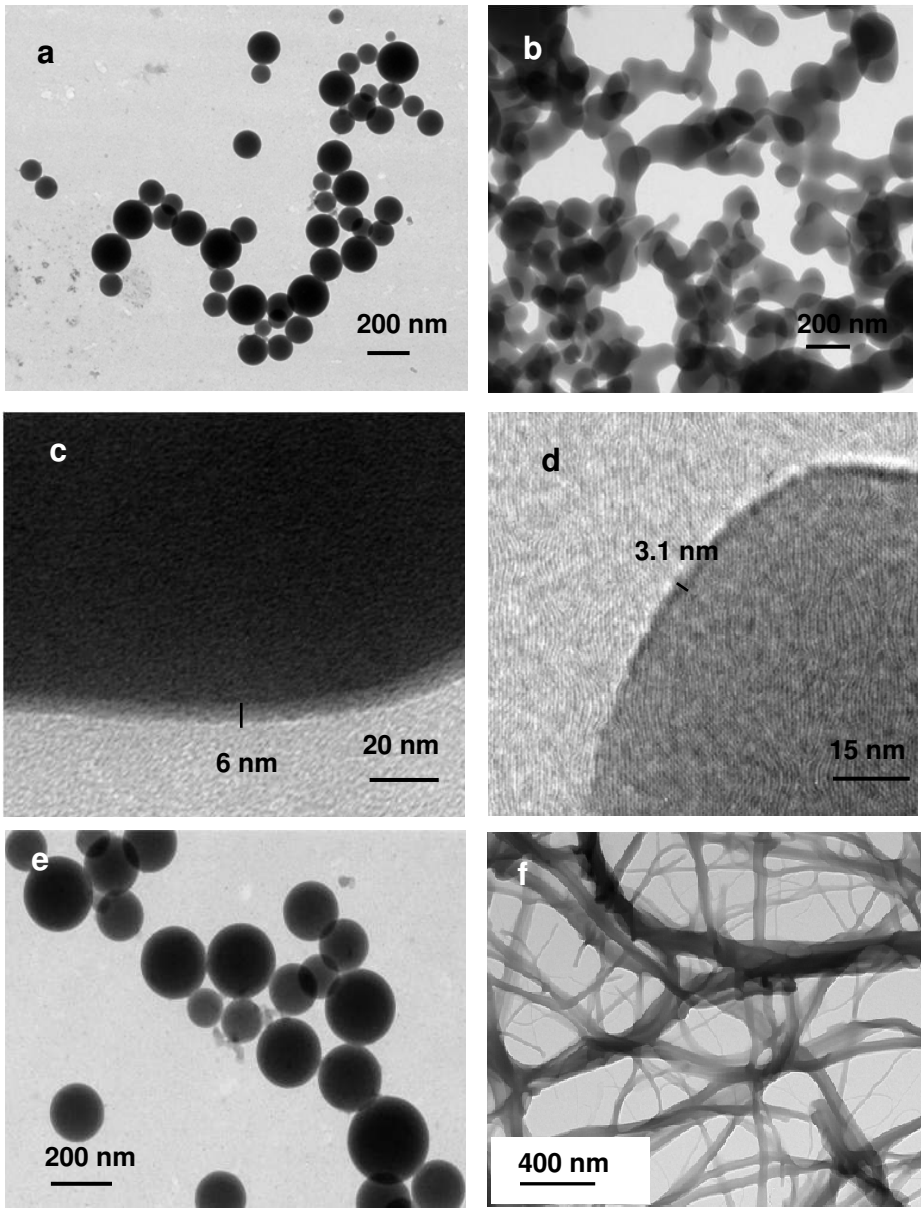

Fig. S13 TEM images of a) compound **IV** in $CHCl_3$-hexane ($1x10^{-5}$ M), b) compound **IV** in $CHCl_3$-hexane ($1x10^{-4}$), c) compound **IV** in $CHCl_3$-hexane ($1x10^{-5}$M) with higher magnification, d) compound **IV** in $CHCl_3$-MeOH ($1x10^{-5}$M) with higher magnification, e) compound **II** from $CHCl_3$-MeOH ($1x10^{-5}$M), and f) xerogel formed from compound **II** in $CHCl_3$-MeOH.

11. Steady state fluorescence spectra

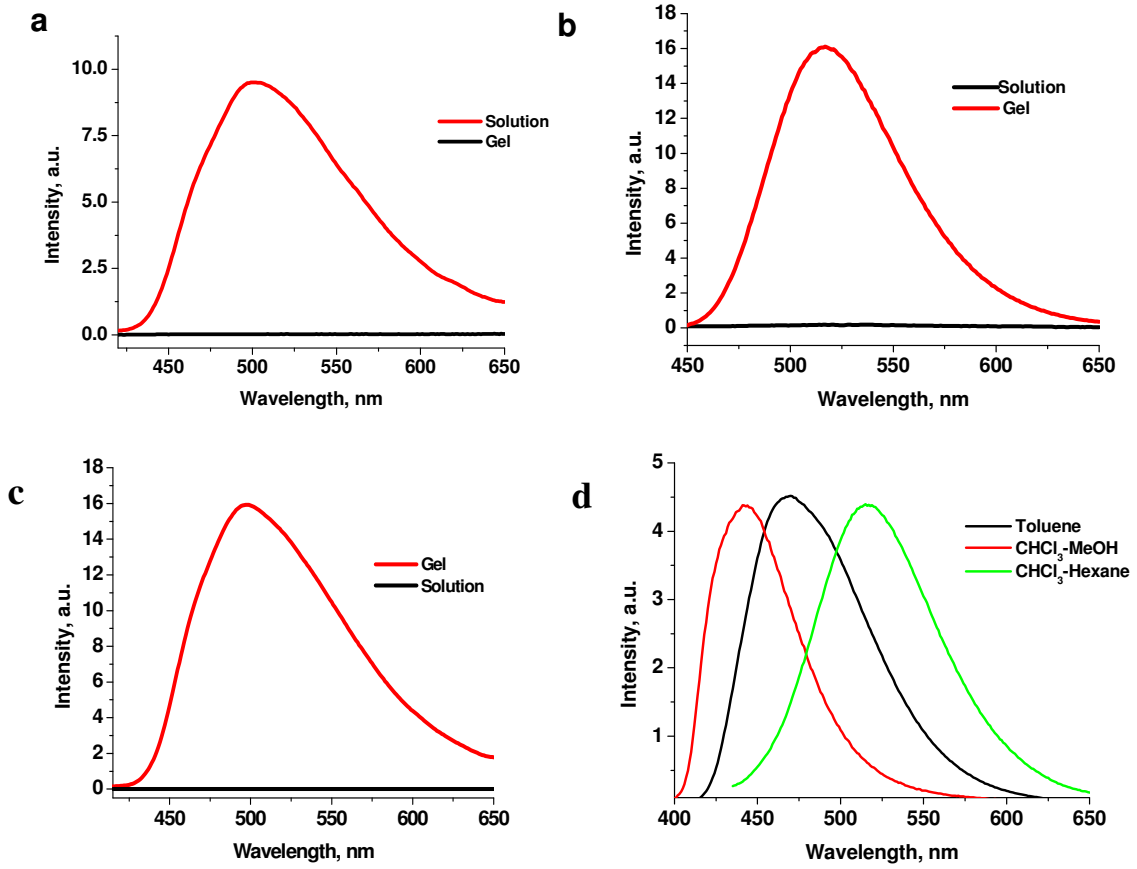

Fig. S14 Emission spectra of compounds **I**, **II**, and **III** in the gel phase (formed from $CHCl_3$) (red traces in a, b and c, respectively), and in $CHCl_3$ solution ($1x10^{-4}$ M) (black traces in a, b and c, respectively). (d) Emission spectra of compound **II** (gel) formed from toluene (black), $CHCl_3$-MeOH (red) and $CHCl_3$-Hexane mixtures.

12. Fluorescence decay trace

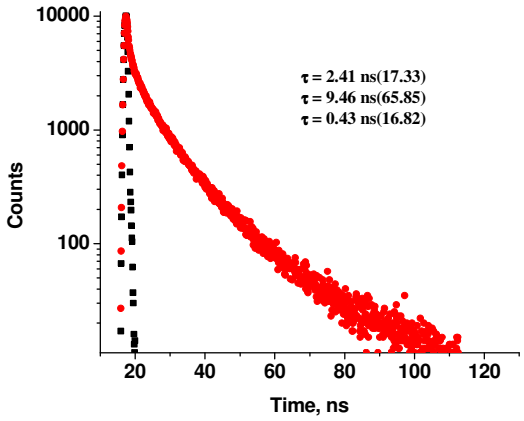

Fig. S15 Fluorescence decay of gel formed from compound **IV** in $CHCl_3$

13. UV-vis absorption spectra of compounds I, II and III in presence of various anions

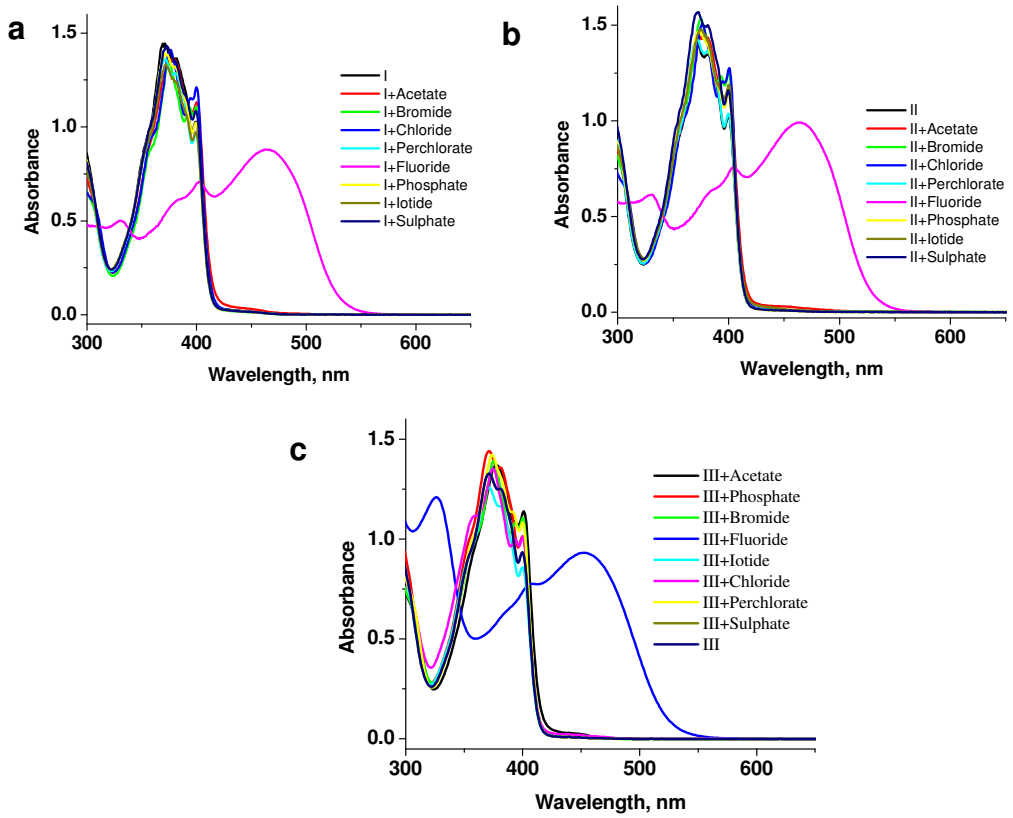

Fig. S16 UV-vis absorption spectra of a) compound **I** (5×10^{-5} M), b) compound **II** (5×10^{-5} M), and c) compound **III** (5×10^{-5} M) in the presence of 1 equiv of various anions in THF.

14. ^{1}HNMR spectra in the presence of and absence of fluoride ion

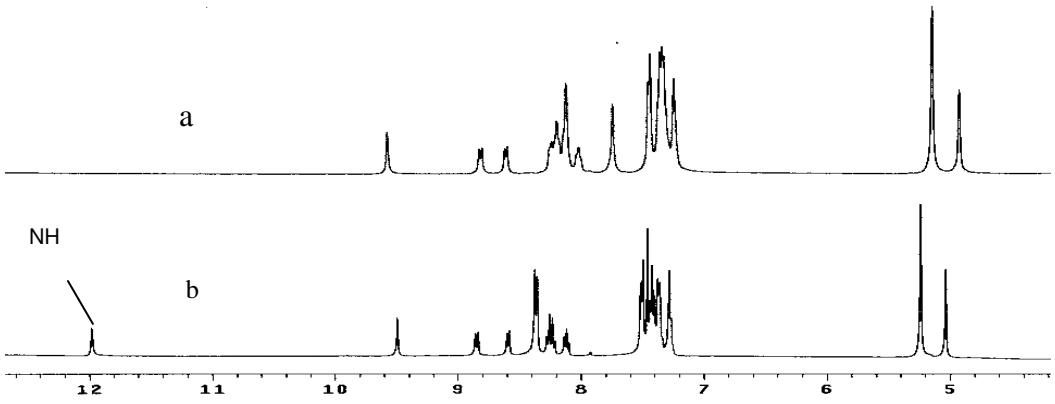

Fig. S17 ^{1}H NMR spectra of compound **I** in DMSO-d_6: (a) in the presence and (b) in the absence of 1 equiv. of F^- ion

16. Reference:

1. P. Rajamalli, E. Prasad, *New J. Chem.* 2011, **35**, 1541-1548.
2. P. Rajamalli, E. Prasad, *Org. Lett.* 2011. **13**, 3714-3717.